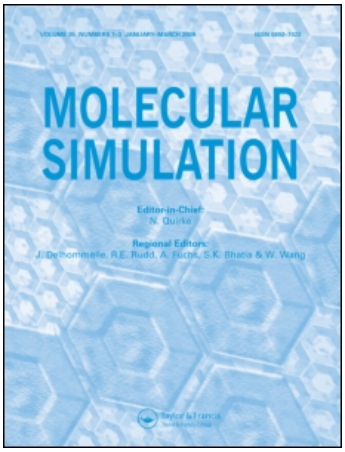

Molecular Simulation
Publication details, including instructions for authors and subscription information:
http://www.informaworld.com/smpp/title~content=t713644482

Studies on binding free energies and the binding mode by docking and MM-PBSA in gp41-ligand complex

J. J. Tan[a]; R. Kong[a]; W. Z. Chen[a]; C. X. Wang[a]
[a] College of Life Sciences and Bioengineering, Beijing University of Technology, Beijing, P.R. China

To cite this Article Tan, J. J. , Kong, R. , Chen, W. Z. and Wang, C. X.(2005) 'Studies on binding free energies and the binding mode by docking and MM-PBSA in gp41-ligand complex', Molecular Simulation, 31: 14, 1051 — 1056
To link to this Article: DOI: 10.1080/08927020500447132
URL: http://dx.doi.org/10.1080/08927020500447132

Molecular Simulation, Vol. 31, No. 14–15, 15–30 December 2005, 1051–1056

Studies on binding free energies and the binding mode by docking and MM-PBSA in gp41-ligand complex

J. J. TAN†, R. KONG‡, W. Z. CHEN¶ and C. X. WANG*

College of Life Sciences and Bioengineering, Beijing University of Technology, Beijing 100022, P.R. China

(Received October 2005; in final form October 2005)

Despite the synthetic peptides inhibit HIV-1 entry, its application may be limited due to the high cost of the peptide production and lack of its oral availability. Thus, it is necessary to identify the small molecule inhibitors reacting with the same or overlapping target sites on gp41 recognizing the antiviral peptides. In this paper, a small inhibitor (*TP1*) is docked into the hydrophobic grooves of gp41 by using Autodock software, resulting in five alternative energetically favorable models. The molecular mechanics-Poisson Boltzmann surface area (MM-PBSA) method is applied to calculate the binding free energies. The data from other studies were used to define our preferred models. We found that only one binding mode is supported by the experimental evidence. The model could be used to design more effective HIV-1 inhibitors targeted to the HIV-1 gp41 core structure.

Keywords: MM-PBSA; Binding free energies; Binding mode; Gp41

1. Introduction

Fusion with the host-cell plasma membrane is crucial stage in the life cycle of HIV, because it is necessary to facilitate the intracellular deposition of the viral genome before replication [1]. The evidence has shown that gp41 undergoes a conformational change upon binding target surface cell receptors, which exposes the hydrophobic N-helical regions (HR-N) and allows the fusion peptides to insert into the host cell membrane [2]. This transient gp41 intermediate then refolds into a stabilized six-helix bundle structure, which brings both the viral and target cell membrane into proximity and results in completion of the fusion process. The fusion-critical helix bundle has been shown by X-ray diffraction data to exist as a gp41 trimer in which the HR-N peptides form a parallel trimeric coiled coil and C-helical regions (HR-C) subsequently pack in an antiparallel fashion into the hydrophobic grooves formed by the coiled coil [3]. Synthetic HR-C and HR-N peptides have been shown to inhibit the fusion, presumably by binding to the prehairpin intermediate and interfering with the formation of the six-helix bundle structure [4,5]. However, orally bioavailable, low molecular weight inhibitors of the process would be preferable and provide a potential platform for drug development against HIV. Therefore, new strategies focusing on the rational design of molecules that recognize protein surfaces could prove fruitful in the development of novel antagonists. Several research groups have screened for inhibitors that specifically target this hydrophobic pocket. Using molecular docking techniques to screen a database of 20,000 organic molecules, Debnath *et al.* [6] found 16 compounds with the best fit for docking into the hydrophobic cavity within the gp41 core and with maximum possible interactions with the target site. Further testing of these compounds by an enzyme-linked immunosorbent assay and virus inhibition assays discerned two compounds (ADS-J1 and ADS-J2) having inhibitory activity at micromolar concentrations on the formation of the gp41 core domain and on HIV-1 infection. Ernst *et al.* [7,8] have also found that trisfunctionalized 3,2′,2″-terphenyl derivatives serve as effective inhibitor to target the gp41.

Wang *et al.* developed molecular mechanics-Poisson Boltzmann solvent accessible surface area (MM-PBSA) and applied the method to predict the activity of inhibitors [9,10] and investigate the binding free energy [11].

†Email: tanjianjun@bjut.edu.cn. Tel.: + 86-10-67392724. Fax: + 86-10-67392837
‡Email: kongren@emails.bjut.edu.cn Tel.: + 86-10-67392724. Fax: + 86-10-67392837
¶Email: wzchen@bjut.edu.cn Tel.: + 86-10-67392724. Fax: + 86-10-67392837
*Corresponding author. Tel.: + 86-10-67392724. Fax: + 86-10-67392837. Email: cxwang@bjut.edu.cn

Molecular Simulation
ISSN 0892-7022 print/ISSN 1029-0435 online © 2005 Taylor & Francis
http://www.tandf.co.uk/journals
DOI: 10.1080/08927020500447132

Compared to the more traditional free energy perturbation simulations, the MM-PBSA method is a slightly less accurate but a considerably faster approach [12]. In this work, the binding free energy (BFE) was calculated by using MM-PBSA. Small inhibitors that bind the hydrophobic pocket would be attractive starting points for developing a new class of small anti-HIV inhibitors; whereas the complex structure of gp41 with small organic molecules has been unknown. Earlier, we have used molecular dynamics (MD) simulation and dock methods, to analysis structure-function relationship between N-terminal region of HIV-1 gp41 and its C-peptide inhibitors [13]. The results showed an interesting correlation with the potency and the α-helical propensity of peptide. In this paper, we present a binding mode of the hydrophobic pocket of gp41 with the terphenyl derivative (*TP1*) by used a flexible docking method (Autodock 3) [14], and will discuss the accuracy of the alternative docking modes for gp41 of HIV-1 in relation to experimental evidence. Then we used MM-PBSA method to calculate the BFE. The calculated free energy by MM-PBSA is almost in accord with the experiment. The binding mode can be used in competitive screens to identify small-molecule drug candidates with similar inhibitory capabilities.

2. Methods

The starting coordinates for the gp41-critical structures were selected from the protein data bank (PDB code 1GZL) [15]. The chemical structure of *TP1* is showed in figure 1. Docking of inhibitors into receptor (N45) was carried out using the Autodock 3.0 program [14]. The inhibitors were placed in the hydrophobic pocket of gp41 for initial position. The Autodock 3.0 program was used to find the best complex conformation and best binding site with a rigid receptor structure. One hundred runs of the space search were carried out to find the best inhibitor–receptor binding mode. MD simulation of the complex (N45–*PL1*) was carried out with the Amber 8 suite of program [16]. The complex was solvated by adding a sphere of TIP3P [17] water molecules with 1.8 nm from all atoms of the complex. The system was first energy minimized for 30,000 steps with the use of the conjugate gradient algorithm. Then, the position-restrained MD simulation was run 0.2 ns. After this, 1 ns MD simulation was carried out at a time step of 2.0 fs and the nonbonded cutoff of 1.2 nm. The SHAKE algorithm [18] was used to constrain bond distances to their equilibrium values in the simulation. Fifty snapshots were collected from the last 0.5 ns simulations for postprocessing analysis.

The binding free energy, ΔG_{bind}, is estimated in this approach from computational analysis of a single simulation of the ligand-bound protein and includes explicit computed components corresponding to "gas-phase" ligand–protein interactions (ΔG_{MM}), conformational entropy ($T\Delta S_{\text{conf}}$), and solvation contributions (ΔG_{solv}):

$$\Delta G_{\text{bind}} = \Delta G_{gas} + \Delta G_{solv} = (\Delta G_{MM} - T\Delta S_{conf}) + \Delta G_{solv} \quad (1)$$

$$\Delta G_{MM} = \Delta G_{\text{int}}^{ele} + \Delta G_{\text{int}}^{VDW} \quad (2)$$

where $\Delta G_{\text{int}}^{\text{ele}}$ and $\Delta G_{\text{int}}^{\text{VDW}}$ denote the electrostatic and van der Walls energetic interactions, respectively.

The solvation free energy in equation (1) can be expressed as:

$$\Delta G_{solv} = \Delta G_{solv}^{ele} + \Delta G_{solv}^{nonpolar} = \Delta G_{PB} + \Delta G_{NP} \quad (3)$$

For each snapshot collected during the simulation, ligand–receptor interaction energies (ΔG_{MM}) and the solvation energies (ΔG_{solv}) were calculated with the MM-PBSA program of Amber 8 (Wang). The configurational/conformational entropy component $T\Delta S_{\text{conf}}$ was estimated from normal model computations by the same snapshots and was computed using the Amber 8 NMODE.

3. Results and discussion

The results obtained by the Autodock 3.0 procedure mentioned above are summarized in table 1. Results differing by less than 0.2 nm of root mean square deviations (rmsd) among each other were grouped into clusters. Of 100 runs, 32 clusters were obtained. Only the top five clusters are shown in table 1, ranked according to the total docking energy E_{total}. That is the sum of the intermolecular energy (E_{inter}) and an estimate of the intramolecular strain (E_{intra}), calculated from the internal van der Waals and electrostatic energies. The docking procedure resulted in five energetically favorable modes for positioning *TP1* in this binding site (see table 1). The mutational analysis indicates that two of the N-helix residues (Leu568 and Trp571) comprising the cavity are critical for membrane fusion activity [19]. Our docking results display that in the other modes except mode **b**

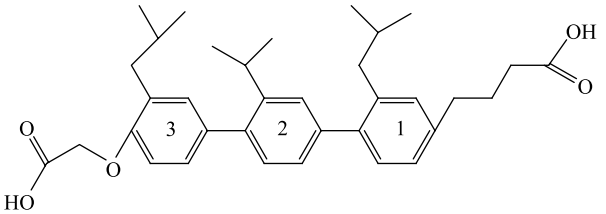

Figure 1. Molecular structure of the compounds studied: 1, benzene ring 1(Ph1); 2, benzene 2(Ph2); 3, benzene 3(Ph3).

Table 1. Overview of the docking results.

Cluster	*N*	E_{inter}	E_{intra}	E_{total}
1	15	−36.42	2.26	−34.16
2	3	−33.66	0.96	−32.69
3	10	−35.87	3.85	−32.02
4	6	−34.53	2.97	−31.56
5	9	−31.60	0.71	−30.89

All energy values are given in kJ/mol.

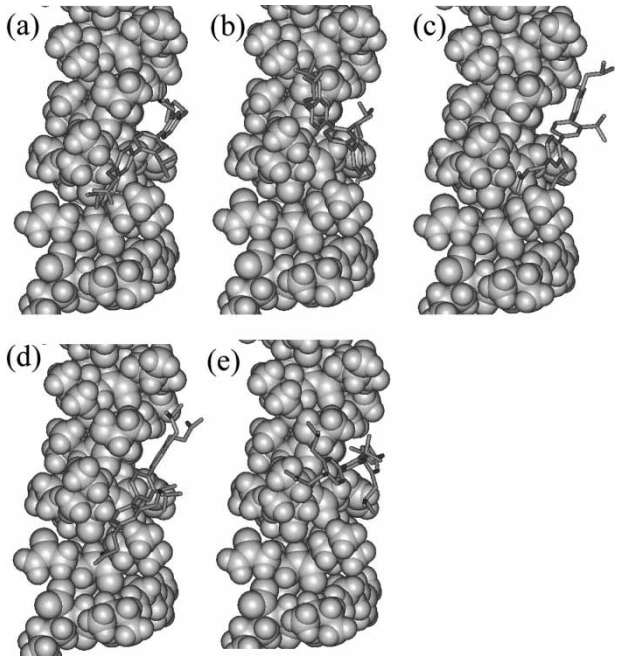

Figure 2. Docking modes for the binding of *TP1* to the gp41 (a–e). Modes **a**–**e**, respectively, of *TP1* docked in the receptor binding site.

(figure 2), the *TP1* is located in the hydrophobic pocket of N45. Chan *et al.* [2] have found that three hydrophobic side chains from the C-helix (Trp628, Trp631, and Ile635) enter deeply into this cavity and are important for the stability of the six-helix bundle and for viral fusion. The X-ray crystal structure of the core structure of the gp41 ectodomain reveals that three N-terminal helices form a central three-stranded coiled coil, whereas three C-terminal helices pack obliquely against the outside of the N36 coiled-coil trimer in an antiparallel orientation [20,21]. Our results show that in mode **a**, **c**, and **d**, *TP1* fills obliquely in the antiparallel orientation into the hydrophobic grooves on the surface of N45. According to information from X-ray crystallography, the hydrophobic pocket is formed by 11 residues on each strand: Leu565, Leu566, Leu568, Thr569, Val570, Trp571, Gly572, Ile573, Lys574, Leu576, and Gln577, and two indole rings from the C-peptide (Trp628 and Trp631) insert into a deep hydrophobic cavity [20]. Our results show that two benzene rings of *TP1* are located in the hydrophobic pocket of N45, in modes (**a**), (**c**)–(**e**).

Hydrophobic interactions (HI) were analyzed using LIGPLOT program [22]. LIGPLOT expresses the hydrophobic interaction as van der Waals contacts involving nonpolar atoms between a ligand and a protein. We use the number of van der Waals contacts of nonpolar atoms (NPA) to represent the hydrophobic interaction strength throughout this paper. The N-peptide residue Ile573 borders the regions of high hydrophobic affinity occupied by Trp631 in the complex of N- and C-peptides[3]. Mutations of Ile573 to hydrophilic residues (Asp, Glu, Gly, and Ser) yield strongly suppressed fusogenic activity, whereas mutations to hydrophobic residues (Leu and Val) have only a small effect, with Ala producing an intermediate phenotype [23]. In modes **a**, **b** and **d**, there are hydrophobic interactions between phenyl rings of *PL1* and Ile573 of N45 (Table 2). In mode **a**, it is eight that the number of the hydrophobic contacts between Ph3 of *PL1* and Ile573 of N45, however, there are only one hydrophobic contact between Ph2 of *PL1* and Ile573 of N45 and three hydrophobic contacts between Ph1 of *PL1* and Ile573 from N45, in mode **d** (table 2). Another small site appears in the indole ring of Trp571 of the N-peptides [24]. The hydrophobic interactions between benzene rings and Trp571 appear in modes **a**, **c**, **d** and **e**. Siebert *et al.* [24] found that Trp-631 is the most tightly bound amino acid in the hydrophobic pocket, having extensive hydrophobic interactions at three sites of the indole ring. Chan *et al.* [25] find that mutation of Trp-631 to Ala dramatically worsens the ability of free C-peptides to inhibit viral entry, increasing the IC_{50} value $\approx$ 30-fold compared to those of wild-type C-peptides. Less dramatic but still substantial effects were seen for mutations of Trp-628 and Ile-635 to Ala, with 5- and 2-fold increases in the IC_{50} values, respectively [25]. In mode **d**, ph2 is the most tightly bound benzene rings in the cavity, because it is the most that NPA between ph2 and hydrophobic pocket (table 2). Figure 3 shows the binding mode between *PL1* and N45 in mode **d**. The interactions between *PL1* and N45 are dominated by the hydrophobic interactions, and the number of the hydrophobic contacts reaches as high as 32 (Table 2). Analysis of the protein-inhibitor interactions

Table 2. The hydrophobic interactions between the N45 and Ph1 or Ph2 or Ph3 in all modes.

Group	*Mode* ***a***		*Mode* ***b***		*Mode* ***c***		*Mode* ***d***		*Mode* ***e***	
	Residue	*Number**	*Residue*	*Number**	*Residue*	*Number**	*residue*	*Number**	*residue*	*Number**
Ph1	Gly572	1	Leu576	2	Gly572	8	Leu576	6	Trp571	4
	Trp571	4	Gly572	8	Thr569	1	Ile573	3	Leu568	5
Ph2	Gly572	7	Ile573	2	Gly572	2	Leu576	1	Gly572	4
	Thr569	4	Gly572	3	Trp571	3	Ile573	1	Thr569	8
			Thr569	6	Leu568	3	Gly572	9	Leu568	2
							Thr569	3		
Ph3	Leu576	2	Thr569	3	Leu568	7	Gly572	2	Thr569	4
	Ile573	8					Trp571	1		
	Gly572	1					Thr569	1		
							Leu568	5		

The hydrophobic interactions with distances of less than 0.35 nm (generated by Ligplot[22]). * The number of hydrophobic contact.

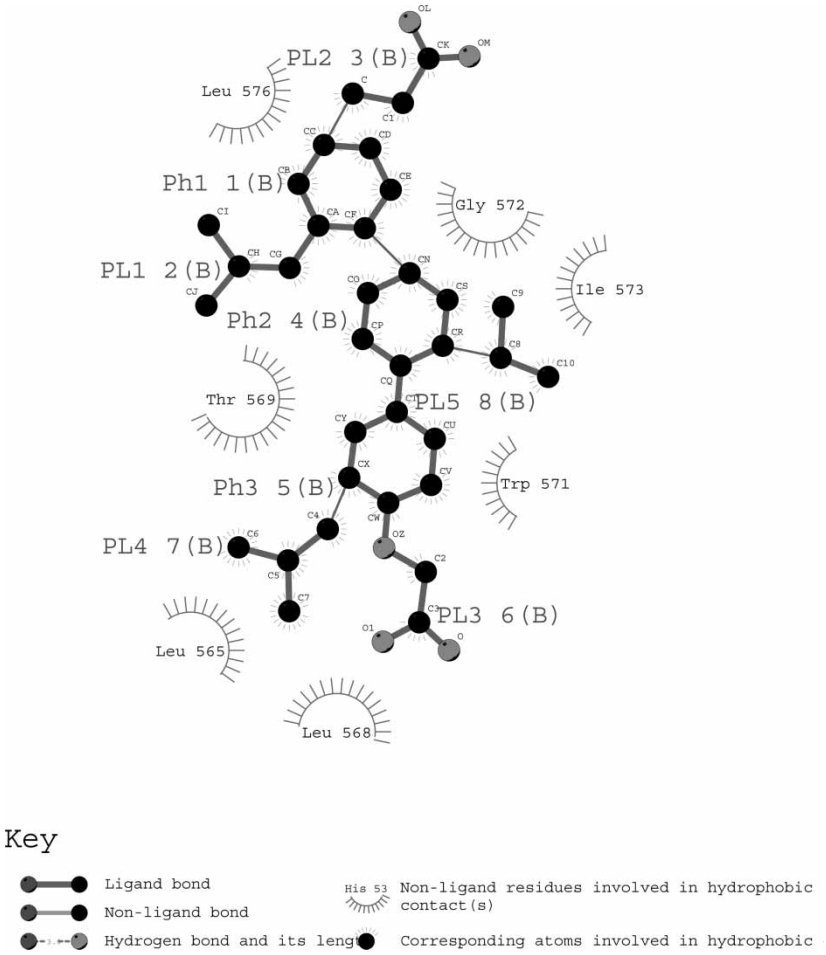

Figure 3. Schematic diagrams showing hydrophobic interactions between *PL1* and N45 in mode **d** obtained by Autodock. Amino acid residues of N45 that have hydrophobic interactions with *PL1* are shown as spiked.

shows that the Gly572, Ile573, Leu576 and Thr569 of N45 are involved in interactions with the benzene rings of *PL1* (figure 3).

The binding free energy between *PL1* and gp41 was calculated with the MM-PBSA method. Examining the free-energy component analysis, we see that the predicted binding free energy is dominated by the van der Walls (Table 3). Otherwise, the value of hydrophobic interaction energy $((\Delta G_{\text{int}}^{\text{VDW}} + \Delta G_{\text{NP}}) = -117.42\,\text{kJ/mol})$ underscores the fact that hydrophobic contributions dominate the binding free energy of gp41 ligand in that they are an order of magnitude greater than the electrostatic contributions. In an examination of the free-energy components in table 3, one notes that the hydrophobic accounts for approximately 98% of the total predicted binding free energy. Its calculated value (ΔG_{calc}) is $-28.13\,\text{kJ/mol}$, somewhat more negative that the ΔG_{expt} of $-25.83\,\text{kJ/mol}$ (table 3). Thus, overall, our data favor the modes **d** since it is supported by experimental evidence. This ability to determine the accuracy of the modes by experimentation is extremely important as has been demonstrated both by the production of two different modes of the gp41, and by the demonstration that the ligand-binding subunits of the receptor may rotate on agonist binding. The generalized Born approach [26] (GB) equation combines the Coulomb and the Born free energy terms and is considerably less computationally demanding than the PB method, but less accurate. However, the GB method represents a compromise between computational simplicity, fast calculation times and precision, making the method more appropriate for qualitative rather than quantitative analysis. Furthermore, energy decomposition is performed for gasphase energies, desolvation free energies calculated with GB, and nonpolar contributions to desolvation using the LCPO method [27]. After MD simulation, there are hydrophobic interaction between

Table 3. Results of free energy calculation by MM-PBSA and NMODE.

$\Delta G_{\text{int}}^{\text{VDW}}$	$\Delta G_{\text{int}}^{\text{ele}}$	ΔG_{PB}	ΔG_{NP}	ΔG_{solv}	$Polar^b$	$Apolar^c$	$T\Delta S$	ΔG_{calc}	$\Delta G_{expt}{}^{\dagger}$
−103.64	−813.59	811.25	−13.77	−119.89	−2.34	−117.42	−89.29	−28.13	−25.83

All energies are in units of kJ/mol. * Polar $= \Delta E_{\text{ele}} + \Delta\Delta G_{\text{PB}}$; apolar $= \Delta E_{vdw} + \Delta\Delta G_{\text{SA}}$. † See Naicker *et al.* and Ernst.

Table 4. Energy contribution of the key residues computed by GB method.

Residue no.[*]	*Polar*	*Apolar*	*Total*
Leu566	0.17	−1.26	−1.09
Gln567	0.75	−0.33	0.42
Leu568	2.47	−6.70	−4.23
Thr569	2.47	−13.35	−10.88
Val570	0.59	−0.84	−0.25
Trp571	1.42	−4.69	−3.27
Gly572	1.51	−7.62	−6.11
Ile573	0.67	−6.91	−6.24
Lys574	−0.54	−0.59	−1.13
Gln575	−4.52	−5.32	−9.84
Leu576	0.63	−8.25	−7.62
Gln577	0.57	−0.33	0.24

All energies are in units of kJ/mol. [*] The residue number are according to the HIV-1 gp160 sequence.

the residue Leu568, Thr569, Gly572, Ile573, Lys574, Gln575, Leu576 of N45 and *PL1* (table 4). Ferrer found Asp632 of the HR-C peptide is in close proximity to Lys574 for ionic interaction and may also play an important role in the stabilization of the sixstranded bundle formed by the HR-N and HR-C fragments in gp41 [28]. A recent mutation study demonstrated that the charged residues in the gp41 coiled-coil domain may also be important for gp41-mediated membrane fusion [29]. Our result shows that there is electrostatic interactions between Lys574 and Gln575 from N45 and PL1 (table 4).

4. Conclusion

The HIV-1 gp41 N-peptide coiled coil offers an attractive target for blocking viral entry into the host cell. During viral fusion, the native C-peptides of gp41 bind into three symmetric grooves on the surface of the transiently exposed N-peptide coiled coil. Within each groove, a prominent hydrophobic pocket has been the focus of drug development efforts. To design potent inhibitors that bind to this large yet shallow groove, it is important to explore the binding mode between small molecule and the cavity. Here, we use Autodock program to find binding mode between small molecule and hydrophobic pocket of gp41 N-peptide. It is found that five alternative energetically favorable models are present. According to the crystallographically determined binding modes of inhibitors and C-peptide complexes, as well as mutation data for N-peptides and inhibition of viral entry by C-peptides, we think that the mode **d** is the most reasonable. The value of computed free energy by MM-PBSA is almost in accord with the value of experiment. In our binding mode, two benzene rings of small molecule inhibitors insert into the cavity of N45, the inhibitors pack obliquely in a parallel orientation, and the N-peptide residue Ile573 has high hydrophobic affinity with the benzene rings of *PL1*. By use of this binding mode, compound databases can then be screened rapidly. Otherwise, the model will be used as foundation to design more effective HIV-1 inhibitors targeted to the hydrophobic pocket of gp41.

Acknowledgements

The authors thank Beijing Natural Science Foundation (No. 5032002 and 5042003) and the Fund from Beijing City Education Committee (No. KZ200410005002) for financial supports.

References

[1] R.A. Lamb. Paramyxovirus fusion—a hypothesis for changes. *Virology*, **197**, 1 (1993).
[2] D.C. Chan, P.S. Kim. HIV entry its inhibition. *Cell*, **93**, 681 (1998).
[3] D.C. Chan, D. Fass, J.M. Berger, P.S. Kim. Core structure of gp41 from the HIV envelope glycoprotein. *Cell*, **89**, 263 (1997).
[4] D.M. Eckert, P.S. Kim. Design of potent inhibitors of HIV-1 entry from the gp41 N-peptide region. *Proc. Natl. Acad. Sci. USA*, **98**, 11187 (2001).
[5] E. Wang, X. Sun, Y. Qian, L. Zhao, P. Tien, G.F. Gao. Both heptad repeats of human respiratory syncytial virus fusion protein are potent inhibitors of viral fusion. *Biochem. Biophys. Res. Commun.*, **302**, 469 (2003).
[6] A.K. Debnath, L. Radigan, S. Jiang. Structure-based identification of small molecule antiviral compounds targeted to the gp41 core structure of the human immunodeficiency virus type 1. *J. Med. Chem.*, **42**, 3203 (1999).
[7] J.T. Ernst, O. Kutzki, A.K. Debnath, S. Jiang, H. Lu, A.D. Hamilton. Design of a protein surface antagonist based on alpha-helix mimicry: inhibition of gp41 assembly and viral fusion. *Angew. Chem. Int. Ed.*, **41**, 278 (2002).
[8] G. Zhou, M. Ferrer, R. Chopra, T.M. Kapoor, T. Strassaier, W. Weissenhorn, J.J. Skehel, D. Oprian, S.L. Shreiber, S.C. Harrison, D.C. Wiley. The structure of an HIV-1 specific cell entry inhibitor in complex with the HIV-1 gp41 trimeric core. *Bioorg. Med. Chem.*, **8**, 2219 (2000).
[9] J. Wang, P. Morin, W. Wang, P.A. Kollmann. Use of MM-PBSA in reproducing the binding free energies to HIV-1 RT of TIBO derivatives and predicting the binding mode to HIV-1 RT of efavirenz by docking and MM-PBSA. *J. Am. Chem. Soc.*, **123**, 5221 (2001).
[10] W. Wang, W.A. Lim, A. Jakalian, J. Wang, R. Luo, C.I. Bayly, P.A. Kollmann. An analysis of the interactions between the Sem-5 SH3 domain and its ligands using molecular dynamics, free energy calculations, and sequence analysis. *J. Am. Chem. Soc.*, **123**, 3986 (2001).
[11] T. Laitinen, J.A. Kankare, M. Peräkylä. Free energy simulations and MM-PBSA analyses on the affinity and specificity of steroid binding to antiestradiol antibody. *Proteins*, **55**, 34 (2004).
[12] B. Kuhn, P.A. Kollman. Binding of a diverse set of ligands to avidin and streptavidin: an accurate quantitative prediction of their relative affinities by a combination of molecular mechanics and continuum solvent models. *J. Med. Chem.*, **43**, 3786 (2000).
[13] J.J. Tan, R. Kong, C.X. Wang, W.Z. Chen. Gp41 hydrophobic pocket entry inhibitor linear interaction energy MD simulation. *J. Mol. Struct. (Theochem)*, **682**, 9 (2004).
[14] G. Jones, P. Willett, R.C. Glen, A.R. Leach, R. Taylor. Development and validation of a genetic algorithm for flexible docking. *J. Mol. Biol.*, **267**, 727 (1997).
[15] S.K. Sia, P.A. Carr, A.G. Cochran, V.N. Malashkevich, P.S. Kim. Short constrained peptides that inhibit HIV-1 entry. *Proc. Natl. Acad. Sci. USA*, **99**, 14664 (2002).
[16] J. Wang, R.M. Wolf, J.W. Caldwell, P.A. Kollman, D.A. Case. Development and testing of a general amber force field. *J. Comput. Chem.*, **25**, 1157 (2004).
[17] W.L. Jorgensen, J. Chandrasekhar, J. Madura, R.W. Impley, M.L. Klein. Comparison of simple potential functions for simulating liquid water. *J. Chem. Phys.*, **79**, 926 (1983).
[18] J.P. Ryckaert, G. Ciccotti, H.J.C. Berendsen. Numerical integration of the cartesian equations of motion of a system with constraints: molecular dynamics of *n*-alkanes. *J. Comput. Phys.*, **23**, 327 (1997).
[19] H.J.C. Berendsen, D. van der Spoel, R. van Drunen. GROMACS: a message-passing parallel molecular dynamics implementation. *Comput. Phys. Commun.*, **91**, 43 (1995).
[20] W. Weissenhorn, A. Dessen, S.C. Harrison, J.J. Skehel, D.C. Wiley. Atomic structure of the ectodomain from HIV-1 gp41. *Nature*, **387**, 426 (1997).

[21] K. Tan, J. Liu, J. Wang, S. Shen, M. Lu. Atomic structure of a thermostable subdomain of HIV-1 gp41. *Proc. Natl. Acad. Sci. USA*, **94**, 12303 (1997).

[22] A.C. Wallace, R.A. Laskowski, J.M. Thornton. LIGPLOT—a program to generate schematic diagrams of protein ligand interactions. *Protein Eng.*, **8**, 127 (1995).

[23] J.W. Dubay, S.J. Roberts, B. Brody, E. Hunter. Mutations in the leucine zipper of the human-immunodeficiency-virus type-1 transmembrane glycoprotein affect fusion and infectivity. *J. Virol.*, **66**, 4748 (1992).

[24] X. Siebert, G. Hummer. Hydrophobicity maps of the N-peptide coiled coil of HIV-1 gp41. *Biochemistry*, **41**, 2956 (2002).

[25] D.C. Chan, C.T. Chutkowski, P.S. Kim. Evidence that a prominent cavity in the coiled coil of HIV type 1 gp41 is an attractive drug target. *Proc. Natl. Acad. Sci. USA*, **95**, 15613 (1998).

[26] R. Constanciel, R. Contreras. Self-consistent field-theory of solvent effects representation by continuum models—introduction of desolvation contribution. *Theor. Chim. Acta*, **65**, 1 (1986).

[27] J. Weiser, P.S. Shenkin, W.C. Still. Approximate atomic surfaces from linear combinations of pairwise overlaps (LCPO). *J. Comput. Chem.*, **20**, 217 (1999).

[28] M. Ferrer, T.M. Kapoor, T. Strassmaier, W. Weissenhorn, J. J. Skehel, D. Oprian, S.L. Schreiber, D.C. Wiley, S.C. Harrison. Selection of gp41-mediated HIV-1 cell entry inhibitors from biased combinatorial libraries of non-natural binding elements. *Nat. Struct. Biol.*, **6**, 953 (1999).

[29] Y.K. Weng, C.D. Weiss. Mutational analysis of residues in the coiled-coil domain of human immunodeficiency virus type 1 transmembrane protein gp41. *J. Virol.*, **72**, 9676 (1998).